Published in final edited form as:
Biochim Biophys Acta. 2013 December ; 1833(12): . doi:10.1016/j.bbamcr.2013.06.015.

The giardial VPS35 retromer subunit is necessary for multimeric complex assembly and interaction with the Vacuolar protein sorting receptor

Silvana L. Miras[1], **María C. Merino**[1], **Natalia Gottig**[2], **Andrea S. Rópolo**[1], and **María C. Touz**[1,*]

[1]Instituto de Investigación Médica Mercedes y Martín Ferreyra, INIMEC – Consejo Nacional de Investigaciones Científicas y Técnicas (CONICET), Universidad Nacional de Córdoba, Córdoba, Argentina

[2]Facultad de Ciencias Bioquímicas y Farmacéuticas, Instituto de Biología Molecular y Celular de Rosario, CONICET, Universidad Nacional de Rosario, Rosario, Argentina

Abstract

The retromer is a pentameric protein complex that mediates the retrograde transport of acid hydrolase receptors between endosomes and the trans-Golgi network and is conserved across all eukaryotes. Unlike other eukaryotes, the endomembrane system of *Giardia* trophozoite is simple and is composed only of the endoplasmic reticulum and peripheral vesicles (PVs), which may represent an ancient organellar system converging compartments such as early and late endosomes and lysosomes. Sorting and trafficking of membrane proteins and soluble hydrolases from the endoplasmic reticulum to the PVs has been described as specific and conserved but whether the giardial retromer participates in receptor recycling remains elusive. Homologs of the retromer Vacuolar Protein Sorting (Vps35p, Vps26p, and Vps29p) have been identified in this parasite. Cloning the GlVPS35 subunit and antisera production enabled the localization of this protein in the PVs as well as in the cytosol. Tagged expression of the subunits was used to demonstrate their association with membranes, and immunofluorescence confocal laser scanning revealed high degrees of colabeling between the retromer subunits and also with the endoplasmic reticulum and PV compartment markers. Protein-protein interaction data revealed interaction between the subunits and of GlVPS35 with the cytosolic domain of the hydrolase receptor GlVps. Altogether our data provide original information on the molecular interactions that mediate assembly of the cargo-selective retromer subcomplex and its involvement in the recycling of the acid hydrolase receptor in this parasite.

Keywords

Giardia lamblia; Retromer; Soluble hydrolase receptor; Endosome; Vacuolar protein sorting

*Corresponding author: Maria Carolina Touz, Instituto de Investigación Médica Mercedes y Martín Ferreyra, INIMEC – CONICET, Friuli 2434, 5000, Córdoba, Argentina. Phone-fax: (54) (351) 468-1465/54-351-4695163. ctouz@immf.uncor.edu.

1.0 Introduction

The retromer complex was first identified in the yeast *Saccharomyces cerevisiae* and can be separated into two subcomplexes: a trimer of Vps35p, Vps29p and Vps26p, which mediates cargo selection and a dimer of Vps5p with Vps17p, which act as the membrane deforming coat [1, 2]. Retromer subunits are highly conserved, with the cargo selective trimer being essentially identical in many eukaryotes, such as mammalian, fly and plant cells [3]. Similar to yeast, the mammalian orthologs of Vps5p and Vps17p, Snx1/Snx2 and Snx5/Snx6, respectively, are members of the sorting nexin (Snx) family, which contains PX (Phox-homology) and BAR (Bin, amphiphysin, Rvs)-motif. PX domains bind to phosphatidylinositol-3-phosphate (PtdIns3P) and other phosphoinositides that are enriched in endosomal membranes [4, 5], whereas BAR domains mediate dimerization and attachment to highly curved membranes [6, 7]. The retromer complex was shown to mediate the recycling of acid hydrolase receptors, like the mammalian mannose 6-phosphate receptor (MPR) or the yeast counterpart Vps10p, from endosomes back to the Golgi [2, 8]. It still unknown whether the recruitment of retromer subcomplexes to the endosomal membrane depends on the recognition of these receptors by Vps35 (or the Vps35–Vps29–Vps26 trimer) or precedes the selection of cargo proteins.

Despite a highly polarized and defined cellular architecture, *Giardia lamblia* has a simplified endomembrane system and lacks key organelles such as a Golgi apparatus, peroxisomes and mitochondria. The basis of this organization is still unclear and a matter of debate (11–18). For instance, there is no agreement on how and where the proteins are secreted and sorted to distinct compartments but there is some consensus that these events may originate in specialized zones of the endoplasmic reticulum (ER) called ER-exit sites [9, 10]. There is general agreement, however, that *Giardia* is a highly adapted eukaryote not only with very low structural and molecular complexity but also with many unusual specializations. Thus, although *Giardia* lacks distinct endosomes and lysosomes, it contains peripheral vacuoles (PVs), which perform the role of endosome and lysosome simultaneously [11–13]. We recently showed that soluble hydrolase acid phosphatase (AcPh) is delivered to the PVs by the concerted action of the giardial receptor Vps (GlVps) and adaptor protein 1 (AP-1) [14] but whether GlVps is later recycled to the ER is still unknown.

The first evidence of retromer-recycling trafficking of GlVps arose from the same work, in which GlVPS35 and GlVps were both precipitated in association with AcPh [14]. However, the interaction between GlVPS35 and GlVps was not tested and remains unknown. Searching the GDB reveals homologs of VPS35, VPS29, and VPS26 (GL50803_23833, GL50803_103855, GL50803_100864) [13]. Although VPS26, VPS29 and VPS35 were reported in *Giardia* as Golgi-associated genes [15], there is no experimental evidence revealing the presence of these proteins. When we modeled the structure of the giardial VPS26 (GlVPS26), it was seen to share a striking similarity with VPS26 from Homo sapiens (Hs). Also, the predicted structure of the giardial small subunit VPS29 and the C-terminal fragment of VPS35 revealed a comparable structure with HsVPS29 and HsVPS35, respectively [13]. Unlike yeast and mammalian cells, no Snx-BAR homologous proteins were obtained after analysis of the GDB, but several predicted proteins showed similarities with partners of the SNX family with PX but not BAR domains, such as SNX3 [4].

This work aimed to characterize the VPS components in the assembly of the cargo-selective retromer subcomplex, define retromer localization, the interaction between the subunits and their involvement in the recycling of the acid hydrolase receptor for continuous cycles of cargo trafficking. Our data provide original information on the molecular interactions that mediate assembly of the cargo-selective retromer subcomplex in *Giardia* and hint at its role as receptor recycler.

Although the best-characterized function of retromer is the regulation of retrograde transport, it has been recently demonstrated that it is also implicated in the trafficking of additional proteins [16–20] strongly suggesting that retromer function is to control diverse membrane trafficking pathways [21]. For instance, it was found by transcriptome analysis in mouse that VPS35 is implicated in Alzheimer's disease [22] and that a VPS26 paralogue in humans (DSCR3) is associated with Down's syndrome [23]. Comparative genomics, cell biology and phylogenetics probed the early evolution of retromer, in which the subunits Vps35, Vps26 and Vps29 were found particularly conserved [3]. In this context, the findings presented here suggest that giardial Vps35, Vps26 and Vps29 conserved the ancient recycling function and support the evolutionary relevance of giardial counterparts. However, further analysis based on these results might also shed light into new and particular function of this complex in *Giardia* and related parasites.

2.0 Materials and methods

2.1 Ethics Statement

The animals (BALB/c mice) bred and maintained at the vivarium of the Instituto Mercedes & Martin Ferreyra (INIMEC-CONICET) have been inspected and approved by the Argentine Department of Animal Care (SENASA). Animal maintenance and care follow the general guidelines provided by The National Institute of Health of the United States of America.

2.2 *Giardia* cell lines and vectors

Trophozoites of the isolate WB, clone 1267 [24] were cultured in TYI-S-33 medium supplemented with 10% adult bovine serum and 0.5 mg/ml bovine bile, as previously described [25]. These trophozoites were used as hosts for the expression of transgenic genes and as wild-type controls. The GlVps open reading frames were amplified from genomic DNA using the primers reported [14]. The GlVPS35 was amplified using the 35F (CATTGGATCCATGGCTTTCCAGACCAAAGTAGACC) and 35R (CATT GCATGC GTTTCCGAGGAAGATCTCCATCCTCT) cloned into the tetracycline-inducible vector pINDG-HA modified by introduction of the HA epitope at the C-terminus to generate the **p**GlVPS-HA vector [26]. After transfection and clone selection, protein expression was induced by the addition of 10 μg/ml of tetracycline to the growth medium. The GlVPS29 open reading frame was amplified from genomic DNA using the 29F (CATTCCATGGCTCAGCAGTTCATTCTCGT) and 29R (CATT GATATCGAATCTTCAAACTTCTTAAGA) primers and the GlVPS26 open reading frame was amplified using the 26F (CATTGGGCCCCTCGGCGGTACAGACACT) and 26R (CATTCCCGGG CGAACCGTACAGACCAGTC) primers. The GlVPS29 and GlVPS26 genes were cloned into **p**TubApaH7pac [27] by restriction and ligation using the *Nco*I and *EcoR*V or *Apa*I and *Sma*I sites, respectively. All sequences were confirmed by sequencing using dye terminator cycle sequencing (Beckman Coulter). Stable trophozoite transfection was performed as previously described [26, 28–31]. All vectors contained a puromycin cassette under the control of the endogenous non-regulated *gdh* promoter for cell selection. Drug-resistant trophozoites were usually apparent by 7–10 days post-transfection. Thus, *glvps35-ha*, *glvps29-ha*, and *glvps26-ha* stably expressing GlVps35-HA, GlVPS29-HA and GlVPS26-HA, respectively, were obtained.

2.3 Antibodies and other reagents

Anti-HA was purchased from Sigma (St. Louis, MO). 9C9 mAb was employed to detect the ER-BiP (Binding immunoglobulin protein) [32]. Anti-μ2 mAb 2F5 was used for the μ2 subunit of AP-2 [33]. 5C1 mAb was used to detect the variant-specific surface protein VSP1267 [34]. Alexa Fluor 488 and 555 was used for the primary antibody label (Zenon

Tricolor Mouse IgG1 Labeling Kit, Molecular Probes, Invitrogen). Mouse polyclonal anti-VPS26 was kindly donated by Dr. Bonifacino [8, 35]. Tween and Triton X-100 were also purchased from SIGMA.

2.4 Reverse transcription polymerase chain reaction (RT-PCR)

The total RNA from wild-type cells was isolated using Trizol reagent (Invitrogen), and a second purification was performed using the SV Total RNA Isolation System (Promega). RT-PCR was performed using the One-step RT-PCR kit (Qiagen, Valencia, CA) as previously described [33]. To determine the expression of sense wild-type mRNA of the three GlVPS cDNA, the 35F/35R, 29F/29R and 26F/26R sets of primers were used. DNA-contamination control (-control) was performed by adding the same primers at the PCR step of the RT-PCR reaction. To control the amounts of RNA loaded into the wells, the expression of the constitutive glutamate dehydrogenase enzyme (GDH) was determined with RT-PCR using the primers GDHf/GDHr [26]. Aliquots (5 μl) of the RT-PCR reaction were size-separated on 1.2% agarose gel in TAE prestained with SYBER SAFE (Invitrogen Corporation, Carlsbad, CA).

2.5 Generation of a polyclonal antibody against GlVPS35

Fusion protein expressing the ORF of giardial VPS35 with thioredoxin tag (pET-32a-m) at its N-terminus was used as immunogen. GlVPS35 fusion protein (100 μg) was emulsified in SIGMA Adjuvant System (SIGMA) and used to intraperitoneally immunize BALB/c mice. Mice were boosted after 21 days with 200 μg of the same preparation. To test the production of anti-GlVPS35 positive polyclonal antibodies (pAb), sera of three immunized mice were analyzed by IFA and immunoblotting (Fig. S1).

2.6 Immunoblot Analysis

Immunoblot assays were performed as previously reported [26]. Briefly, 10 μg of total proteins were incubated with sample buffer, boiled for 10 min, and separated in 10% Bis-Tris gels. Samples were transferred to nitrocellulose membranes, blocked with 5% skimmed milk and 0.1% Tween 20 in TBS, and then incubated with primary antibody diluted in the same buffer. After washing and incubation with an enzyme-conjugated secondary antibody, proteins were visualized with the SuperSignal West Pico Chemiluminescent Substrate (Pierce, Thermo Fisher Scientific Inc., Rockford, IL, USA) and autoradiography. Controls included the omission of the primary antibody, the use of an unrelated antibody, or assays using non-transfected cells.

2.7 Immunofluorescence assays

For immunofluorescence assays of fixed cells, trophozoites cultured in growth medium were harvested and processed as described [14]. For direct double staining, the anti-HA mAb (Sigma, St. Louis, MO) was labeled with Zenon Alexa Fluor 488 and was used to detect HA-tagged GlVPSs (final dilution of anti-HA 1:500), while 9C9, 2F5 mAbs and anti-GlVPS35 were labeled with Zenon Alexa Fluor 555 (1:200 final dilution), following the suggested protocol (Zenon Tricolor Mouse IgG1 Labeling Kit, Molecular Probes, Invitrogen Corporation, Carlsbad, CA). Controls included the omission of the primary antibody and the staining of wild-type cells. Fluorescence staining was visualized with a motorized FV1000 Olympus confocal microscope (Olympus UK Ltd, UK), using 63× or 100× oil immersion objectives (NA 1.32). The fluorochromes were excited using an argon laser at 488 nm and a krypton laser at 568 nm. Detector slits were configured to minimize any cross-talk between the channels. Differential interference contrast images were collected simultaneously with the fluorescence images, by the use of a transmitted light detector. Images were processed using FV10-ASW 1.4 Viewer and Adobe Photoshop 8.0 (Adobe Systems) software. The

colocalization and deconvolution were performed using MetaMorph software (Molecular Devices, Silicon Valley, CA). 2D blind deconvolution, when applied, was set with the following parameters: Total iteration ≤ 5, PSF correction factor of 2, and Super resolution factor of 1.

2.8 Quantitative colocalization analysis (QCA)

Confocal immunofluorescence microscopy and quantitative colocalization analysis were performed using the Fiji image processing package (http://fiji.sc/wiki/index.php/Fiji) over raw images. Background was corrected using the threshold value for all channels to remove background and noise levels completely. The Pearson's correlation coefficient (PC) and the Mander's overlap coefficient (M) were examined. PC values range between −1.0 and 1.0, where 0 indicates no significant correlation and −1.0 indicates complete negative correlation. The M values are in the range from 0 to 1.0. If the image has an overlap coefficient of 0.5, it implies that 50% of both its objects, i.e. pixels, overlap. A value of zero means that there are no overlapping pixels. This coefficient is not sensitive to the limitations of typical fluorescence imaging [36–39]. PC values indicating colocalization range from 0.5 to 1.0 while for the M colocalization is considered in the range from 0.6 to 1.0.

2.9 Subcellular Fractionation Procedures

Same amount (1×10^9 cells) of *wild-type Giardia* trophozoites and trophozoites expressing GlVPS29-HA or GlVPS26-HA were harvested, washed twice in ice-cold PBS, homogenized, and resuspended in 1.0 ml of 250 mM sucrose containing the Complete Protease Inhibitor Cocktail (Roche). The lysates were then sonicated three times at 4°C (30 s, 20 A, in a VCX 130 Sonic Disruptor) and centrifuged at 1,000 x g for 10 min to remove unbroken cells and nuclei. A centrifugal force of 1000 x g (P1), 20.000 x g (P2), and 105.000 x g (P3) were then layered on a discontinuous sucrose gradient formed by layering 750 μl of 60, 55, 50, 45, 40, 35, 30, and 25% (w/w) sucrose into an SW 40 polyallomer centrifuge tube. The gradient was centrifuged for 18 h at 100,000 x g and fractionated from the top into 7 fractions (**1** to **7**). Protein content in each fraction was measured with the Qubit® Protein Assay Kit (Invitrogen). For Dot-blotting, 10 μg of each fraction were diluted with PBS to 1 ml, and proteins were precipitated by addition of 250 μl of concentrated trichloroacetic acid. Precipitated proteins were collected by centrifugation at 10,000 x g for 10 min, washed once with acetone, and air dried for 1 h at room temperature. Dried and washed protein pellets were redissolved in 30 μl of SDS-PAGE sample buffer, boiled for 3 min and 10 μl dotted to nitrocellulose, and probed with 9C9 mAb to detect the ER-Bip protein [32], anti-μ2 mAb 2F5 for PVs fractions [40] and 5C1 mAb to detect VSP1267 [34].

2.10 Membrane fractionation

Fractionation was carried out according to Schröter et al. with minor modifications [41]. All procedures were carried out at 4°C or ice. 10 mM Tris acetate buffer, pH 7.0, containing 250 mM sucrose with protease inhibitor was used as a fractionation buffer throughout the procedure. The cells were harvested by centrifugation at 500 x g for 10 min and washed three times. The cell pellet was suspended in 0.3 ml of buffer and homogenized by ultrasonic treatment (5 pulses of 5 J) (Vibra Cell; Sonics and Materials Inc., Ct. USA). The cell homogenate was then centrifuged at 8,000 x g for 10 min to isolate plasma membranes and nuclei (fraction P1). The supernatant was again centrifuged at 130,000 x g for 60 min to remove microsomes (fraction P2). The final supernatant contained highly purified cytosol (SN). All pellets were washed with fractionation buffer and centrifuged again. The supernatants of the washing steps were discarded.

2.11 Yeast-two hybrid assay (YTH)

The MATCHMAKER Two-hybrid system was used following the manufacturer's suggested protocol (Clontech, Palo Alto, CA). The two-hybrid pGBKT7(TRP1) vector (GAL4 DNA binding domain, BD) containing the gene for GlVPS35 was used as bait, while GlVPS29 and GlVPS26 genes were ligated to the pGADT7-Rec(LEU2) vector (GAL4 transcription activation domain, AD), yielding GlVPS35-BD, GlVPS29-AD, and GlVPS26-AD vectors, respectively. AH109 transformants were cultured at 30°C for 4–5 days on plates with minimal medium lacking leucine and tryptophan (-L/-T) to test for positive transformation, or in the absence of leucine, tryptophan, and histidine (TDO – triple dropout medium), to study specific protein interactions as previously described [28]. High-stringency medium that also lacked adenine (QDO) was also used to test strong protein-protein interactions. Controls included the pESCP-AD/pμ1-BD interaction (protein-protein interaction control) [28, 42] and the **p**GlVPS35-BD/ pGADT7 empty vector (autoactivation control).

2.12 Immunoprecipitation assay (IPP)

Transgenic *Giardia* trophozoites were harvested and resuspended in 1 ml of cold lysis buffer (300 mM NaCl, 1% Triton X-100, mM EDTA and protease inhibitors cocktail) for 1 h at 4°C. The lysate was centrifuged at 10 000 g for 10 min at 4°C, and the supernatant mixed with anti-VPS35 or anti-hVPS26 and incubated overnight at 4°C. Protein L-agarose beads (50 ml; Qiagen, Valencia, CA) were added to each sample and incubated for 4 h at 4°C. Beads were pelleted at 700 g and washed four times with washing buffer (50 mM NaH_2PO_4, pH 8.0; 300 mM NaCl; 0.1% Triton X-100). Beads were resuspended in sample buffer and boiled for 10 min before immunoblot analysis using HRP-labeled anti-HA mAb. Control included testing of transgenic cells without addition of antibody. Also, wild-type cells and a non-related mAb were used as controls of these assays.

3.0 Results

3.1 Expression of GlVPS35, GlVPS29 and GlVPS26

The cargo-selective subcomplex components GlVPS35, GlVPS26 and GlVPS29 of the putative *Giardia* retromer were previously described [13, 15]. Three dimensional analyses using structural modeling have shown that GlVPS26 have structural homology to arrestin while GlVPS29 possesses a globular α/β topology with a central β-sandwich surrounded by α-helices [13]. The structure of the C-terminal fragment of GlVPS35 was modelled using the VPS29-VPS35 crystal model from human proteins showing a curved all α-helical structure (Fig. 1) [13]. BLAST searches in the *Giardia* database (GDB) for sequences homologous to yeast or human retromer proteins were unable to define homologs to the Vps5/17 or SNXs subcomplexes but several proteins containing PX domains with no BAR-motif were found (see discussion).

To learn more about the core subcomplex in *Giardia*, the mRNA expression of the subunits was first analyzed by reverse-transcriptase PCR assays showing that all of them were expressed in the trophozoite stage (Fig. 2A). Confocal microscopy revealed a localization of Hemaglutinin (HA)-tagged GlVPS35 consistent with the PVs area besides the cytosol in *glvps35-ha* transgenic trophozoites (Fig. 2B, top panel). Also, it was observed a clear localization of GlVPS35 in the bare zone (BZ), a cytoplasmic protrusion located between the nuclei containing vacuoles that are presumed to be identical to the PVs [12, 14, 28, 43]. The molecular mass of GlVPS35-HA observed by immunoblotting matched exactly the predicted mass of ~85 kDa (Fig. 2C, top panel). Polyclonal antibodies were generated against recombinant GlVPS35 and tested on *glvps35-ha* and *wild-type* trophozoites by immunoblot and immunofluorescence assays (Fig. 2C and Fig. S1). Native GlVPS35 showed the same subcellular localization and expression of GlVPS35-HA in trophozoites,

suggesting that the over-expression of this subunit neither affects its distribution nor has any influence in its molecular mass (Fig. 2C and S1). Over-expression of HA-tagged GlVPS29 and GlVPS26 exhibited diffuse cytoplasmic staining in *glvps29-ha* and *glvps26-ha* transgenic trophozoites, respectively, with multiple distinct punctate labeling patterns consistent with the ER localization (Fig. 2B, middle and bottom panels). The observed molecular weights of GlVPS29-HA and GlVPS26-HA were ~45 kDa and ~60 kDa, respectively (Fig. 2C, middle and bottom panels). Testing anti-human VPS26 antiserum (mVPS26) [35], a cross-reaction was observed with the corresponding protein in *wild-type* and *glvps26-ha* trophozoites (Fig. 2C). Although no clear staining pattern was observed in *wild-type* or *glvps26-ha* trophozoites in IFA using the mVPS26, it was able to coimmunprecipitate GlVPS26-HA from *glvps26-ha* trophozoites (not shown). With these tools, it was possible to further characterize the assembly and distribution of the cargo-selective retromer subcomplex.

3.2 GlVPS subunits are concentrated in specific organelles

Retromer location was explored by performing immunofluorescence microscopy on *wild-type* or transgenic *glvps29-ha* and *glvps26-ha* trophozoites. As seen in Figure 3A and B, there was low colocalization between GlVPS35 and the ER marker BiP [32] but a substantial colocalization with the PV marker AP-2 [12]. A greater colocalization of GlVPS26-HA and GlVPS29-HA with BiP was obtained when *glvps29-ha* and *glvps26-ha* transgenic trophozoites were analyzed, with a reduced degree of colocalization when these proteins were costained with anti-AP-2 (Fig. 3A and B). In all the images, deconvolution was applied to sharpen the membrane localization of these subunits. All these results were convincingly underscored by statistical analysis with Pearson's correlation coefficient (PC) and Mander's overlap coefficient (M). 2D scattergram of the green/red pair of channels did not show any pixels concentrated at the diagonal of the scattergram for GlVPS35/BiP but an increase of the representation of yellow (colocalized) pixels along the diagonal was observed for GlVPS29-HA/BiP and GlVPS26-HA/BiP pairs (Fig. 3A). The increase of the degree of colocalization between GlVPS29-HA or GlVPS26-HA with BiP was estimated by the PC and M coefficients, with values close to 1.0 indicating significant correlation. When the retromer subunits and AP-2 colocalization were assessed, the 2D scattergram showed a greater correlation for all subunits (Fig. 3B) with PC and M coefficients over 0.7 in all cases.

For further evidence of retromer localization, sedimentation velocity analyses were performed on linear sucrose gradients of each subunit and compared with VSP1267, BiP and AP-2, markers for plasma membrane (PM), ER and PVs, respectively. As in the case of the colocalization analyses described above, GlVPS35, GlVPS26-HA, and GlVPS29-HA were found in both PV and ER-associated pools (Fig. 4). Lower amounts of GlVPS35 were also detected in regions of the gradient containing the VSP1267 protein located at the plasma membrane, as was the case for human Vps35 [44]. If GlVPS35 is recruited to the PV membrane by the receptor and acts as the platform for retromer assembly, then binding of GlVPS26 and GlVPS29 may subsequently occur, thus explaining the differences in retromer protein localization.

3.3 *Giardia* retromer is membrane-associated

Schröter et al.'s fractionation protocol [41] was followed to determine the subcellular distribution of retromer. Homogenates of *wild-type* and transgenic trophozoites were subjected to sequential centrifugations at 8,000 *x g* and 130,000 *x g*, yielding the P1 (plasma membrane and nuclei), P2 (microsome), and SN (cytosol) fractions (Fig. 5A). These three fractions were subjected to protein gel blotting with anti-GlVPS35 or anti-HA, for GlVPS35 and GlVPS29-HA/GlVPS26-HA respectively, showing that GlVPS35 was present primarily in the microsomal fraction, with a lower amount detectable in the cytosol fraction. By

contrast, equal amounts of GlVPS29-HA and GlVPS26-HA were detected in the membrane and soluble fraction (Fig. 5B). This closely resembles the distribution of Vps35p, Vps29p, and Vps26p in the corresponding fractions from yeast [2, 45].

To analyze the association of the retromer complex subunits, the colocalization between GlVPS35 with GlVPS29-HA and GlVPS26-HA was examined in *glvps29-ha* or *glvps26-ha* transgenic cells. Immunofluorescence and deconvoluted images indicated that GlVPS35 and GlVPS29-HA proteins exhibited a discrete punctate located below the plasma membrane (Fig. 5C), the region of the cell in which the PVs are located. The same pattern of colocalization in the PVs was observed between GlVPS35 and GlVPS26-HA (Fig. 5C). Also, some colocalization of GlVPS35 with GlVPS26-HA in the BZ was observed. Although the colocalization in both cases was partial, results of the correlation analysis for the staining intensity of both antibodies expressed as Pearson's and Mander's correlation coefficients showed a direct correlation of 0.637 and 0.702 with an average colocalization of 88.9% and 93.8% for the pairs GlVPS35/GlVPS29-HA and GlVPS35/GlVPS26-HA, respectively. This trend may indicate that the cargo-selective retromer subcomplex of the retromer is assembled at the PV membrane. Moreover, since GlVPS35/GlVPS26-HA colocalized in the BZ, it is possible that the cargo-assemble subcomplex occurs also at this area, similar to what happens in the PVs.

3.4 Assembly of the cargo-selective retromer subcomplex

Structural study suggests that VPS29 and VPS26 bind to VPS35 independently of each other, with no direct contact between the two subunits, and the association of one does not enhance the binding of the other [46, 47]. To examine whether a similar complex is formed in *Giardia* trophozoites, an analysis was conducted using the MATCHMAKER Two-hybrid system, which is especially suited for the detection of low and high affinity interactions. Colony growth assays showed that GlVPS35 strongly interacted with GlVPS29 and GlVPS26 (Fig. 6A). No interactions were observed when these constructs were replaced by empty-AD vectors, indicating that there is no autoactivation. No interaction was detected either between the GlVPS29 and GlVPS26 by YTH (result not shown). Similar results were obtained in immunoprecipitation (IPP) assays. Transgenic *glvps29-ha*, *glvps26-ha* or *wild-type* cells were lysed and the GlVPS35 protein immunoprecipitated using the anti-GlVPS35 pAb. Immunoblotting showed that GlVPS29-HA and GlVPS26-HA were coimmunoprecipitated together with GlVPS35 only in transgenic cells (Fig. 6B). These results not only confirmed the binary interactions between the GlVPS subunits but also showed that the GlVPS29-HA and GlVPS26-HA overexpressed proteins were able to be assembled into the cargo-selective retromer subcomplex.

Giardial VPS35 exhibits, similarly to yeast, *C. elegans* and human Vps35, a completely conserved PRLYL motif contained within an amino-terminal domain (Fig. 6C). This conserved motif was shown to be essential for the interaction between VPS35 and VPS26, with the arginine residue being determinant for their association [48]. The present study examined the ability of the $_{122}$PRLYL$_{126}$ conserved amino-terminal domain of GlVPS35 to interact with the GlVPS26 subunit of the giardial retromer complex. By YTH, this conserved N-terminal domain was established as responsible for GlVPS35 binding to GlVPS26, as only GlVPS35$_{1–765}$ (whole protein) or GlVPS35$_{1–448}$ (N-terminus of GlVPS35) showed strong interaction with GlVPS26 (Fig. 6C). Moreover, GlVPS35-GlVPS26 interaction was observed to be dependent upon the presence of the entire $_{122}$PRLYL$_{126}$ motif as no association was observed when this motif was site-mutated (Fig. 6C). As shown by the YTH assay, GlVPS26 associated with GlVPS35-HA but was unable to interact with GlVPS35$_{126–765}$, the GlVPS35 version lacking the N-terminus and the $_{122}$PRLYL$_{126}$ motif, when IPP assays were performed (Fig. 6D). For these assays, *glvps35-ha* or *wild-type* cells were lysated and native GlVPS26 immunoprecipitated by

using the mVPS26 pAb. No interaction between the N- or C-terminus of GlVPS35 alone was observed for GlVPS29 (not shown). Altogether, these results suggest that a special conformational status of GlVPS35, and not only a specific residue, might be determinant at the time of defining the interaction of GlVPS35 with the other two subunits.

3.5 Cargo recognition of GlVPS35

Biochemical analyses identified GlVPS35 and the receptor GlVps as being associated with the soluble hydrolase AcPh [14]. This result prompted us to determine whether there is a direct interaction between GlVPS35 and GlVps. Immunofluorescence and confocal microscopy with antibodies to GlVPS35 and GlVps-HA, showed a distinct staining but similar punctate colocalization in region between the PVs and ER in *glvps-ha* transgenic trophozoites (Fig. 7A). Colony growth in YTH assays showed that GlVPS35 and GlVps do interact, although it seems to be a low affinity interaction (Fig. 7B). Interestingly, addition of anti-GlVps35 pAb to the homogenate of *glvps-ha* transgenic cells (stably expressing GlVps-HA), allowed the coprecipitation of GlVps-HA and GlVps35 (Fig. 7B). Thus, these experiments showed GlVPS35 as the cargo recognition component of the *Giardia* retromer able to bind the hydrolase receptor, probably to recycle it.

4.0 Discussion

It has been extensively demonstrated that the retromer complex is well conserved throughout its eukaryotic lineage, suggesting an ancient origin and an analogous coat function to those of COPI, COPII and clathrin vesicles [2, 49]. The cargo-selective subcomplex, composed of Vps26, Vps29 and Vps35, is present in all eukaryotes examined so far [3], but this is not true for all the retromer-interacting proteins [21]. Thus, the characterization of the retromer complex in different organisms may reveal novel roles in diverse cellular processes and/or intracellular trafficking routes. Due to its simplified organellar organization, *Giardia* may provide the basic rules required for retromer-mediated protein sorting, including endosome-to-Golgi retrieval. This work describes three giardial retromer proteins, GlVPS35, GlVPS29, and GlVPS26, defines their localization within the cell, the protein-protein interactions that allow them to assemble into a multimeric complex and sets the basis for the retromer role in PV-to-ER recycling of soluble hydrolase receptor in this parasite.

Analysis of the primary sequence showed that GlVPS35 is extremely well conserved [3]. However, GlVPS29 has an unusual long extension in the C-terminal that differs from other eukaryotes (Fig. S2). It was shown that Vps29p *S. cerevisiae* also contains an additional ~80 amino acid loop, when compare with mammals, responsible for the greater affinity observed with Vps5p [50]. It is possible that, similar to Vps29 from other species, the extra C-terminal of GlVPS29 might be a scaffold for retromer interaction with accessory proteins [51]. Also, GlVPS29 and GlVPS26 C-terminus showed variability between *Giardia* assembles (e.g A, E and B) that may account for additional roles of these subunits in each parasite. On the other hand, when the 3D structure of the conserved domains was analyzed, a high degree of structural similarity of GlVPS35, GlVPS29 and GlVPS26 subunits with their orthologs in humans and rat was found [13]. This conservation was evident when we found that a polyclonal mouse antibody raised against the human VPS26 subunit was also able to recognize GlVPS26 in immunoblot and immunoprecipitation assays. When the subcellular localization of native or HA-tagged subunits was analyzed, a unique localization was observed in addition to their cytoplasmic distribution, with GlVPS35 mainly located in the PVs while GlVPS29 and GlVPS26 was found concentrated in the ER. We envisage that the cargo-selective retromer subcomplex functions in *Giardia* primarily based on its ability to regulate retrograde transport, but it is possible that the differential subcellular distribution

observed between the GlVPSs reveals the participation of each protein alone in different cellular processes, as was reported for other cells [reviewed in [52]].

Although the analysis of cytosolic and microsomal fractions both contained GlVPS35, GlVPS29, and GlVPS26, the partial colocalization of these subunits in PV-like structures distributed alongside the plasma membrane, suggests that the multimeric complex might be assembled at the PV membrane and not in the cytosol (see below). When total proteins were immunoadsorbed by the anti-GlVPS35 antibody, GlVPS29-HA and GlVPS26-HA were coprecipitated, demonstrating that these proteins physiologically form a multimeric complex. Based on the two-hybrid data and the immunolocalization and immunoprecipitation studies, we favor the interpretation that GlVPS35 is at the core of the complex and subsequently bound to GlVPS26 and GlVPS29. In yeast, Vps35p can extend along the deformed membrane, interacting with Vps26 and Vps29 at each end [53]. In the case of Vps29p, its metallophosphoesterase site may provide a scaffold for the C-terminal half of Vps35p binding [53–55] while Vps26p binds to the N-terminal end of Vps35p through a loop and contiguous residues at its C-terminal domain [46, 56]. The data from the two-hybrid analysis of the interactions between GlVPS35 and GlVPS26 agrees with the data obtained from the studies in yeast. We were able to determine that the N-terminal tail of GlVPS35 interacted with GlVPS26 and this association involved the recognition of a conserved $_{122}$PRLYL$_{126}$ motif present at N-terminal domain of GlVPS35. However, while the interaction between this conserved amino-terminal domain is entirely dependent upon the presence of R107 (the functional equivalent of R98 in yeast Vps35p) in the human VPS35, the entire motif seems to be critical for GlVPS35 and GlVPS26 interaction. Deletion of the N-terminus or mutation of each of the $_{122}$PRLYL$_{126}$ conserved residues resulted in a GlVPS35 mutant that cannot bind to GLVPS26. On the other hand, neither the N- nor the C-terminus of GLVPS35 alone was able to interact with GLVPS29, showing that binding to GlVPS29 appears to be dependent on the integrity of the GlVPS35 conformation. Still, it is not clear whether assembly of the cargo-selective retromer subcomplex takes place sequentially on the endosomal membrane or if it is recruited to the membrane after previous assembly as a unit in the cytosol, but it is predicted to be aligned parallel to the membrane, allowing GlVPS35 to interact with cargo proteins.

How the interaction of GlVPS35 with cargo is regulated deserves detailed examination. The human VPS35 subunit can interact with the cytoplasmic tail of Cation-Independent MPR, and genetic studies in yeast strongly support a direct role for Vps35p in cargo binding [8, 57]. In a previous report, we showed that a membrane protein named GlVps serves as the sorting receptor for the soluble hydrolase AcPh. GlVps transport AcPh from the ER-exit sites to the PVs via its interaction with the AP-1 adaptor protein. To maintain the forward flow of hydrolases to the PVs, GlVps must be efficiently recycled back to the ER-exit site and reused in additional rounds of hydrolase sorting. The participation of retromer in the selection and binding of GlVps was determined by the ability of GlVPS35 to interact with the cargo receptor. GlVps-HA and the native GlVPS35 colocalized partially in the PVs but also in the reticular structure around the nuclei, suggesting that cargo recognition may take place in the PVs with the recycling traffic ended at the ER-sorting station. Because failure to retrieve the receptor may result in its rapid degradation and the missorting of AcPh, further studies aimed at disclosing the motif involved in GlVps-GlVPS35 interaction and function are needed.

None of the proteins that comprise the cargo-selective complex in *Giardia* contains a known lipid-binding domain and it is unclear how the cargo-selective complex is recruited to the membrane. It has been postulated that the Snx-BAR dimer may recruit the cargo recognition subcomplex to the endosomal membrane and subsequently drive tubule formation [5, 8, 58]. Also, the small GTPase Rab7a was shown to be required for recruitment of the cargo-

selective trimer in *Entamoeba*, yeast and humans [59–61] and, recently, other proteins like SNX3 (Snx with PX but not BAR domain) have been implicated in mediating the recruitment of the cargo-selective retromer complex [62]. Analyzing the presence of Snx-BAR homologous proteins in the *Giardia* genome, we found SNX-like proteins that have no BAR domain but contain a PX domain. From all the giardial proteins containing the PX domain, only two of them fulfilled the requirements for SNX-like protein, such as the absence of signal peptide or transmembrane domain, and their homology with no-BAR SNX proteins like SNX15 and SNX17 [63, 64]; Miras & Touz, unpublished results]. Interestingly, a polyclonal antibody anti-human SNX1 [8, 44] recognized two trophozoite proteins of 30 and 120 kDA MWs which matched the predicted giardial SNX homologous to SNX15 and SNX17, respectively [63, 64]; Miras & Touz, unpublished results]. It is thus possible that these two giardial SNXs, like SNX3, may play a role in the recruitment of the retromer cargo-selective retromer subcomplex to the PVs. However, since they do not have a recognizable BAR domain, no tubule formation may occur which is consistent with the absence of tubules in ultrastructural images of *Giardia* trophozoites. Moreover, there are no clear orthologs of Rab7, which regulate retromer function in more complex cells, and thus how the cargo-selective retromer subcomplex is recruited and interacts with PV membranes will be a matter of extensive analysis.

All the results obtained here prompted us to propose a hypothetical model in which GlVPS35, GlVPS29, GlVPS26, and non-BAR sorting nexins (GlSNXs) are involved in the retrieval of the GlVps receptor from the PVs to the ER in *Giardia* (Fig. 8). In this model, the recruitment of GlVPS35 to the PV membranes may occur alongside direct association with the GlVps receptor. The association of GlVPS26 may be also required for cargo recognition, as its structure was found to be similar to the endocytic adaptor protein arrestin and was repeatedly located in the PVs together with GlVPS35. This would promote or stabilize the association of GlVPS35 to the membrane, thus affecting the interaction with the receptor. While GlVPS35 serves as the platform for the formation of the cargo-selective retromer subcomplex, VPS29 may be required for stabilizing the retromer complex by its binding to GlVPS35. On the other hand, we speculate that GlSNXs may act as a scaffold for the correct membrane association of the GlVPS35, which is constitutively bonded to the PVs. Finally, oligomerization of the subcomplexes into budding domains could serve to promote clustering of the complex and the receptor retrieval process. Further evidence of the function on the non-BAR GlSNXs, incapable of performing tubulation by themselves, are required to disclose whether they may function together with the cargo-selective subcomplex as an heteropentamer or rather as two independent subcomplexes for PV-to-ER receptor retrieval as suggested by Harbour et al. [50, 51].

The findings presented in this work support the established function of the cargo-selective retromer subcomplex in endosome-to-Golgi receptor recycling. However, the different localization of each subunit together with the absence of Snx-BAR proteins may indicate additional roles of this complex. Although the retromer is conserved across all eukaryotes, studies of the retromer in mammalian and yeast cells revealed some differences involving the complex's stability and its association with dissimilar proteins [3]. The diverse roles played by these proteins alone or as a complex possibly depend on the requirements of each organism. Therefore, the analysis of the retromer and retromer-accessory proteins from diverse eukaryotes will have important consequences for our understanding of retromer-mediated sorting, developing a more complete understanding of how it works.

Supplementary Material

Refer to Web version on PubMed Central for supplementary material.

Acknowledgments

We thank Dr. Juan Bonifacino for their kind gift of anti-mVPS26 pAb. The project was supported by Grant Number R01TW00724 from the Fogarty International Center. The content is solely the responsibility of the authors and does not necessarily represent the official views of the Fogarty International Center or the National Institutes of Health. This research was also supported in part by the Argentine Agencia Nacional para la Promoción de la Ciencia y Tecnología (FONCyT- PICT2010-737). NG, ASR and MCT are researchers from the National Council of Research (CONICET). SLM is a PhD fellow from CONICET. MCM is postdoctoral fellow from FONCyT.

References

1. Seaman MN, Marcusson EG, Cereghino JL, Emr SD. Endosome to Golgi retrieval of the vacuolar protein sorting receptor, Vps10p, requires the function of the VPS29, VPS30, and VPS35 gene products. J Cell Biol. 1997; 137:79–92. [PubMed: 9105038]
2. Seaman MN, McCaffery JM, Emr SD. A membrane coat complex essential for endosome-to-Golgi retrograde transport in yeast. J Cell Biol. 1998; 142:665–681. [PubMed: 9700157]
3. Koumandou VL, Klute MJ, Herman EK, Nunez-Miguel R, Dacks JB, Field MC. Evolutionary reconstruction of the retromer complex and its function in Trypanosoma brucei. J Cell Sci. 2011; 124:1496–1509. [PubMed: 21502137]
4. Yu JW, Lemmon MA. All phox homology (PX) domains from Saccharomyces cerevisiae specifically recognize phosphatidylinositol 3-phosphate. J Biol Chem. 2001; 276:44179–44184. [PubMed: 11557775]
5. Rojas R, Kametaka S, Haft CR, Bonifacino JS. Interchangeable but essential functions of SNX1 and SNX2 in the association of retromer with endosomes and the trafficking of mannose 6-phosphate receptors. Mol Cell Biol. 2007; 27:1112–1124. [PubMed: 17101778]
6. Carlton J, Bujny M, Peter BJ, Oorschot VM, Rutherford A, Mellor H, Klumperman J, McMahon HT, Cullen PJ. Sorting nexin-1 mediates tubular endosome-to-TGN transport through coincidence sensing of high- curvature membranes and 3-phosphoinositides. Curr Biol. 2004; 14:1791–1800. [PubMed: 15498486]
7. Peter BJ, Kent HM, Mills IG, Vallis Y, Butler PJ, Evans PR, McMahon HT. BAR domains as sensors of membrane curvature: the amphiphysin BAR structure. Science. 2004; 303:495–499. [PubMed: 14645856]
8. Arighi CN, Hartnell LM, Aguilar RC, Haft CR, Bonifacino JS. Role of the mammalian retromer in sorting of the cation-independent mannose 6-phosphate receptor. J Cell Biol. 2004; 165:123–133. [PubMed: 15078903]
9. Faso C, Hehl AB. Membrane trafficking and organelle biogenesis in Giardia lamblia: Use it or lose it. Int J Parasitol. 2011
10. Faso C, Konrad C, Schraner EM, Hehl AB. Export of cyst wall material and Golgi organelle neogenesis in Giardia lamblia depend on endoplasmic reticulum exit sites. Cell Microbiol. 2012
11. Lanfredi-Rangel A, Attias M, de Carvalho TM, Kattenbach WM, De Souza W. The peripheral vesicles of trophozoites of the primitive protozoan Giardia lamblia may correspond to early and late endosomes and to lysosomes. J Struct Biol. 1998; 123:225–235. [PubMed: 9878577]
12. Rivero MR, Vranych CV, Bisbal M, Maletto BA, Ropolo AS, Touz MC. Adaptor protein 2 regulates receptor-mediated endocytosis and cyst formation in Giardia lamblia. Biochem J. 2010; 428:33–45. [PubMed: 20199400]
13. Touz MC, Rivero MR, Miras SL, Bonifacino JS. Lysosomal Protein Trafficking in *Giardia lamblia*. Common and Distinct Features Front Biosci (Elite Ed). 2012; 4:1898–1909.
14. Rivero MR, Miras SL, Feliziani C, Zamponi N, Quiroga R, Hayes SF, Ropolo AS, Touz MC. Vacuolar Protein Sorting Receptor in Giardia lamblia. PLoS One. 2012; 7:e43712. [PubMed: 22916299]
15. Dacks JB, Davis LA, Sjogren AM, Andersson JO, Roger AJ, Doolittle WF. Evidence for Golgi bodies in proposed 'Golgi-lacking' lineages. Proc Biol Sci. 2003; 270(Suppl 2):S168–171. [PubMed: 14667372]

16. Verges M, Luton F, Gruber C, Tiemann F, Reinders LG, Huang L, Burlingame AL, Haft CR, Mostov KE. The mammalian retromer regulates transcytosis of the polymeric immunoglobulin receptor. Nat Cell Biol. 2004; 6:763–769. [PubMed: 15247922]

17. Strochlic TI, Setty TG, Sitaram A, Burd CG. Grd19/Snx3p functions as a cargo-specific adapter for retromer-dependent endocytic recycling. J Cell Biol. 2007; 177:115–125. [PubMed: 17420293]

18. Eaton S. Retromer retrieves wntless. Dev Cell. 2008; 14:4–6. [PubMed: 18194646]

19. Popoff V, Mardones GA, Tenza D, Rojas R, Lamaze C, Bonifacino JS, Raposo G, Johannes L. The retromer complex and clathrin define an early endosomal retrograde exit site. J Cell Sci. 2007; 120:2022–2031. [PubMed: 17550971]

20. Chen D, Xiao H, Zhang K, Wang B, Gao Z, Jian Y, Qi X, Sun J, Miao L, Yang C. Retromer is required for apoptotic cell clearance by phagocytic receptor recycling. Science. 2010; 327:1261–1264. [PubMed: 20133524]

21. Seaman MN. The retromer complex - endosomal protein recycling and beyond. J Cell Sci. 2012; 125:4693–4702. [PubMed: 23148298]

22. Small SA, Kent K, Pierce A, Leung C, Kang MS, Okada H, Honig L, Vonsattel JP, Kim TW. Model-guided microarray implicates the retromer complex in Alzheimer's disease. Ann Neurol. 2005; 58:909–919. [PubMed: 16315276]

23. Hu YH, Warnatz HJ, Vanhecke D, Wagner F, Fiebitz A, Thamm S, Kahlem P, Lehrach H, Yaspo ML, Janitz M. Cell array-based intracellular localization screening reveals novel functional features of human chromosome 21 proteins. BMC Genomics. 2006; 7:155. [PubMed: 16780588]

24. Nash TE, Aggarwal A, Adam RD, Conrad JT, Merritt JW Jr. Antigenic variation in Giardia lamblia. J Immunol. 1988; 141:636–641. [PubMed: 2454999]

25. Keister DB. Axenic culture of Giardia lamblia in TYI-S-33 medium supplemented with bile. Trans R Soc Trop Med Hyg. 1983; 77:487–488. [PubMed: 6636276]

26. Touz MC, Conrad JT, Nash TE. A novel palmitoyl acyl transferase controls surface protein palmitoylation and cytotoxicity in Giardia lamblia. Mol Microbiol. 2005; 58:999–1011. [PubMed: 16262786]

27. Touz MC, Lujan HD, Hayes SF, Nash TE. Sorting of encystation-specific cysteine protease to lysosome-like peripheral vacuoles in Giardia lamblia requires a conserved tyrosine-based motif. J Biol Chem. 2003; 278:6420–6426. [PubMed: 12466276]

28. Touz MC, Kulakova L, Nash TE. Adaptor protein complex 1 mediates the transport of lysosomal proteins from a Golgi-like organelle to peripheral vacuoles in the primitive eukaryote Giardia lamblia. Mol Biol Cell. 2004; 15:3053–3060. [PubMed: 15107467]

29. Elmendorf HG, Singer SM, Nash TE. The abundance of sterile transcripts in Giardia lamblia. Nucleic Acids Res. 2001; 29:4674–4683. [PubMed: 11713317]

30. Singer SM, Yee J, Nash TE. Episomal and integrated maintenance of foreign DNA in Giardia lamblia. Mol Biochem Parasitol. 1998; 92:59–69. [PubMed: 9574910]

31. Yee J, Nash TE. Transient transfection and expression of firefly luciferase in Giardia lamblia. Proc Natl Acad Sci U S A. 1995; 92:5615–5619. [PubMed: 7777558]

32. Lujan HD, Mowatt MR, Conrad JT, Nash TE. Increased expression of the molecular chaperone BiP/GRP78 during the differentiation of a primitive eukaryote. Biol Cell. 1996; 86:11–18. [PubMed: 8688827]

33. Rivero MR, Vranych CV, Bisbal M, Maletto BA, Ropolo AS, Touz MC. Adaptor Protein 2 Regulates Receptor-Mediated Endocytosis and Cyst Formation in Giardia lamblia. Biochem J. 2010

34. Nash TE, Conrad JT, Mowatt MR. Giardia lamblia: identification and characterization of a variant-specific surface protein gene family. J Eukaryot Microbiol. 1995; 42:604–609. [PubMed: 7581335]

35. Haft CR, de la Luz Sierra M, Barr VA, Haft DH, Taylor SI. Identification of a family of sorting nexin molecules and characterization of their association with receptors. Mol Cell Biol. 1998; 18:7278–7287. [PubMed: 9819414]

36. Zinchuk V, Zinchuk O, Okada T. Quantitative colocalization analysis of multicolor confocal immunofluorescence microscopy images: pushing pixels to explore biological phenomena. Acta Histochem Cytochem. 2007; 40:101–111. [PubMed: 17898874]

37. Garcia Penarrubia P, Ferez Ruiz X, Galvez J. Quantitative analysis of the factors that affect the determination of colocalization coefficients in dual-color confocal images. IEEE Trans Image Process. 2005; 14:1151–1158. [PubMed: 16121462]
38. Sun H, Crossland WJ. Quantitative assessment of localization and colocalization of glutamate, aspartate, glycine, and GABA immunoreactivity in the chick retina. Anat Rec. 2000; 260:158–179. [PubMed: 10993953]
39. Zhu C, Barker RJ, Hunter AW, Zhang Y, Jourdan J, Gourdie RG. Quantitative analysis of ZO-1 colocalization with Cx43 gap junction plaques in cultures of rat neonatal cardiomyocytes. Microsc Microanal. 2005; 11:244–248. [PubMed: 16060977]
40. Nash TE, Conrad JT, Merritt JW Jr. Variant specific epitopes of Giardia lamblia. Mol Biochem Parasitol. 1990; 42:125–132. [PubMed: 1700296]
41. Schroter CJ, Braun M, Englert J, Beck H, Schmid H, Kalbacher H. A rapid method to separate endosomes from lysosomal contents using differential centrifugation and hypotonic lysis of lysosomes. J Immunol Methods. 1999; 227:161–168. [PubMed: 10485263]
42. Rivero MR, Miras SL, Quiroga R, Ropolo AS, Touz MC. Giardia lamblia low-density lipoprotein receptor-related protein is involved in selective lipoprotein endocytosis and parasite replication. Mol Microbiol. 2011; 79:1204–1219. [PubMed: 21205007]
43. House SA, Richter DJ, Pham JK, Dawson SC. Giardia flagellar motility is not directly required to maintain attachment to surfaces. PLoS Pathog. 2011; 7:e1002167. [PubMed: 21829364]
44. Haft CR, de la Luz Sierra M, Bafford R, Lesniak MA, Barr VA, Taylor SI. Human orthologs of yeast vacuolar protein sorting proteins Vps26, 29, and 35: assembly into multimeric complexes. Mol Biol Cell. 2000; 11:4105–4116. [PubMed: 11102511]
45. Paravicini G, Horazdovsky BF, Emr SD. Alternative pathways for the sorting of soluble vacuolar proteins in yeast: a vps35 null mutant missorts and secretes only a subset of vacuolar hydrolases. Mol Biol Cell. 1992; 3:415–427. [PubMed: 1498362]
46. Shi H, Rojas R, Bonifacino JS, Hurley JH. The retromer subunit Vps26 has an arrestin fold and binds Vps35 through its C-terminal domain. Nat Struct Mol Biol. 2006; 13:540–548. [PubMed: 16732284]
47. Norwood SJ, Shaw DJ, Cowieson NP, Owen DJ, Teasdale RD, Collins BM. Assembly and solution structure of the core retromer protein complex. Traffic. 2011; 12:56–71. [PubMed: 20875039]
48. Zhao X, Nothwehr S, Lara-Lemus R, Zhang BY, Peter H, Arvan P. Dominant-negative behavior of mammalian Vps35 in yeast requires a conserved PRLYL motif involved in retromer assembly. Traffic. 2007; 8:1829–1840. [PubMed: 17916227]
49. Wassmer T, Attar N, Harterink M, van Weering JR, Traer CJ, Oakley J, Goud B, Stephens DJ, Verkade P, Korswagen HC, Cullen PJ. The retromer coat complex coordinates endosomal sorting and dynein-mediated transport, with carrier recognition by the trans-Golgi network. Dev Cell. 2009; 17:110–122. [PubMed: 19619496]
50. Harbour ME, Seaman MN. Evolutionary variations of VPS29, and their implications for the heteropentameric model of retromer. Commun Integr Biol. 2011; 4:619–622. [PubMed: 22046480]
51. Harbour ME, Breusegem SY, Antrobus R, Freeman C, Reid E, Seaman MN. The cargo-selective retromer complex is a recruiting hub for protein complexes that regulate endosomal tubule dynamics. J Cell Sci. 2010; 123:3703–3717. [PubMed: 20923837]
52. Verges M. Retromer: multipurpose sorting and specialization in polarized transport. Int Rev Cell Mol Biol. 2008; 271:153–198. [PubMed: 19081543]
53. Hierro A, Rojas AL, Rojas R, Murthy N, Effantin G, Kajava AV, Steven AC, Bonifacino JS, Hurley JH. Functional architecture of the retromer cargo-recognition complex. Nature. 2007; 449:1063–1067. [PubMed: 17891154]
54. Collins BM, Skinner CF, Watson PJ, Seaman MN, Owen DJ. Vps29 has a phosphoesterase fold that acts as a protein interaction scaffold for retromer assembly. Nat Struct Mol Biol. 2005; 12:594–602. [PubMed: 15965486]

55. Damen E, Krieger E, Nielsen JE, Eygensteyn J, van Leeuwen JE. The human Vps29 retromer component is a metallo-phosphoesterase for a cation-independent mannose 6-phosphate receptor substrate peptide. Biochem J. 2006; 398:399–409. [PubMed: 16737443]
56. Collins BM, Norwood SJ, Kerr MC, Mahony D, Seaman MN, Teasdale RD, Owen DJ. Structure of Vps26B and mapping of its interaction with the retromer protein complex. Traffic. 2008; 9:366–379. [PubMed: 18088321]
57. Nothwehr SF, Ha SA, Bruinsma P. Sorting of yeast membrane proteins into an endosome-to-Golgi pathway involves direct interaction of their cytosolic domains with Vps35p. J Cell Biol. 2000; 151:297–310. [PubMed: 11038177]
58. Bonifacino JS, Hurley JH. Retromer. Curr Opin Cell Biol. 2008; 20:427–436. [PubMed: 18472259]
59. Rojas R, van Vlijmen T, Mardones GA, Prabhu Y, Rojas AL, Mohammed S, Heck AJ, Raposo G, van der Sluijs P, Bonifacino JS. Regulation of retromer recruitment to endosomes by sequential action of Rab5 and Rab7. J Cell Biol. 2008; 183:513–526. [PubMed: 18981234]
60. Nakada-Tsukui K, Saito-Nakano Y, Ali V, Nozaki T. A retromerlike complex is a novel Rab7 effector that is involved in the transport of the virulence factor cysteine protease in the enteric protozoan parasite Entamoeba histolytica. Mol Biol Cell. 2005; 16:5294–5303. [PubMed: 16120649]
61. Seaman MN, Harbour ME, Tattersall D, Read E, Bright N. Membrane recruitment of the cargo-selective retromer subcomplex is catalysed by the small GTPase Rab7 and inhibited by the Rab-GAP TBC1D5. J Cell Sci. 2009; 122:2371–2382. [PubMed: 19531583]
62. Harterink M, Port F, Lorenowicz MJ, McGough IJ, Silhankova M, Betist MC, van Weering JR, van Heesbeen RG, Middelkoop TC, Basler K, Cullen PJ, Korswagen HC. A SNX3-dependent retromer pathway mediates retrograde transport of the Wnt sorting receptor Wntless and is required for Wnt secretion. Nat Cell Biol. 13:914–923. [PubMed: 21725319]
63. Phillips SA, Barr VA, Haft DH, Taylor SI, Haft CR. Identification and characterization of SNX15, a novel sorting nexin involved in protein trafficking. J Biol Chem. 2001; 276:5074–5084. [PubMed: 11085978]
64. van Kerkhof P, Lee J, McCormick L, Tetrault E, Lu W, Schoenfish M, Oorschot V, Strous GJ, Klumperman J, Bu G. Sorting nexin 17 facilitates LRP recycling in the early endosome. EMBO J. 2005; 24:2851–2861. [PubMed: 16052210]

Highlights

- A conformational organization of GlVPS35, GlVPS26 and GlVPS29 components of the giardial retromer is proposed.
- GlVPS35, GlVPS26 and GlVPS29 subunits are concentrated in the ER and lysosomal vacuoles.
- GlVPS35, GlVPS29, GlVPS26 are membrane-associated.
- The assembly of the cargo-selective retromer subcomplex depends on GlVPS35.
- GlVPS35 might be clustered by its binding to the hydrolase receptor.

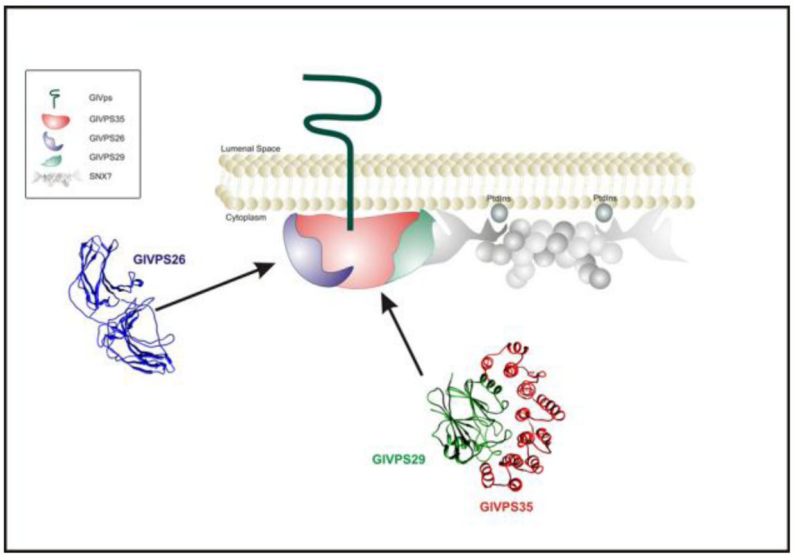

Figure 1. Postulated organization of the giardial retromer complex and its interactions

GlVPS35 interacts with the cargo GlVps. GlVPS35 also interacts with GlVPS26 through its N-terminus and with GlVPS29 through its C- terminus at the membrane of the PVs. 3D structures of the cargo-selective complex are depicted [13]. Sortinexin (SNX) may contribute to the membrane attachment through recognition of specific PtdIns.

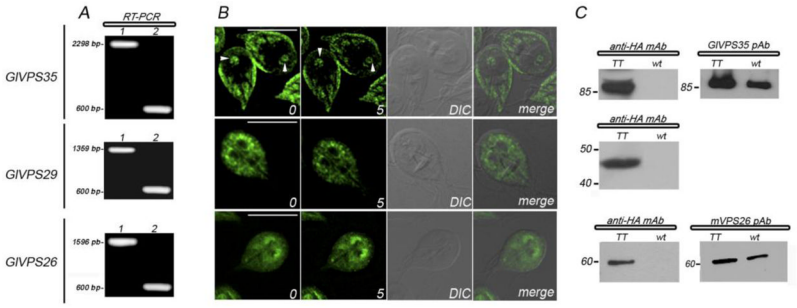

Figure 2. Expression of the cargo-selective retromer subcomplex proteins

(A) RT-PCR experiments show that the mRNA of GlVPS35, GlVPS29, and GlVPS26 are expressed as predicted by the GiardiaDB. 1: ORF for each subunit (*glvps35*: 2298 bp, *glvps29* 1359 bp, and *glvps26* 1596 bp). 2: expression of a glutamate dehydrogenase (*gdh*) mRNA fragment (600 bp) was tested as positive control. DNA-contamination control was performed (not shown). (B) IFA and confocal microscopy of the HA-tagged GlVPS subunits present a single focal plane selected from a three-dimensional stack of optical sections, before processing (0 iteration) and after deconvolution (5 iterations). The three subunits show cytoplasmic localization (0) but GlVPS35-HA is observed close to the plasma membrane and in the bare zone between the nuclei (arrowheads), while GlVPS29 and GlVPS26 mainly localized around the nuclei in deconvoluted pictures (5). DIC: Differential interference contrast microscopy. Merges of DIC and deconvoluted images are shown. Bar, 10 μm. (C) On the left, immunoblot assays using anti-HA mAb show the predicted bands for GlVPS35-HA, GlVPS29-HA, and GlVPS26-HA in transgenic trophozoites (TT) but not in *wild-type* cells (wt). On the right, anti-GlVPS35 pAb was able to detect the native GlVPS35 in both *glvps35-ha* TT and wt cells. The same occurred when the anti-mVPS26 pAb was tested in *glvps26-ha* TT and wt cells. Molecular weights of protein standards (kDa) are indicated on the left.

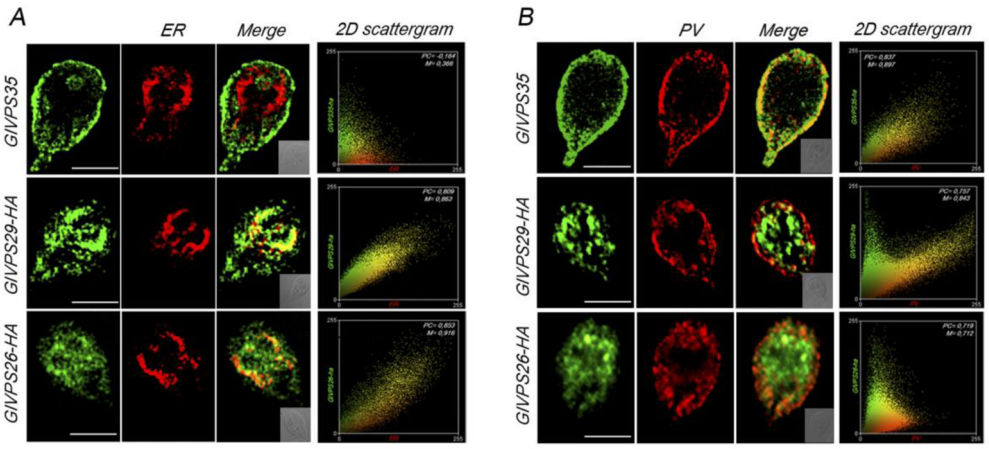

Figure 3. Subcellular distribution of GlVPS35, GlVPS29 and GlVPS26

(A) Direct IFA and confocal microscopy show that GlVPS35 (green) does not colocalize with the ER-resident chaperone BiP (red) in the ER. 2D scattergrams of the two labels denote the lack of colocalization (right panel). GlVPS29-HA and GlVPS26-HA (green) largely colocalize with BiP as observed in yellow in the merged pictures and 2D scattergram. Pearson's coefficient (PC). Mander's Overlap coefficient (M). Bar, 10 μm. (B) Direct IFA and confocal microscopy images show massive localization of GlVPS35 but highly reduced presence of GlVPS29-HA and GlVPS26-HA in the PVs. Differential interference contrast microscopy is shown as insert. 2D scattergram (panels on the right) correspond to the colocalization analysis. Pearson's coefficient (PC). Mander's Overlap coefficient (M). Bar, 10 μm.

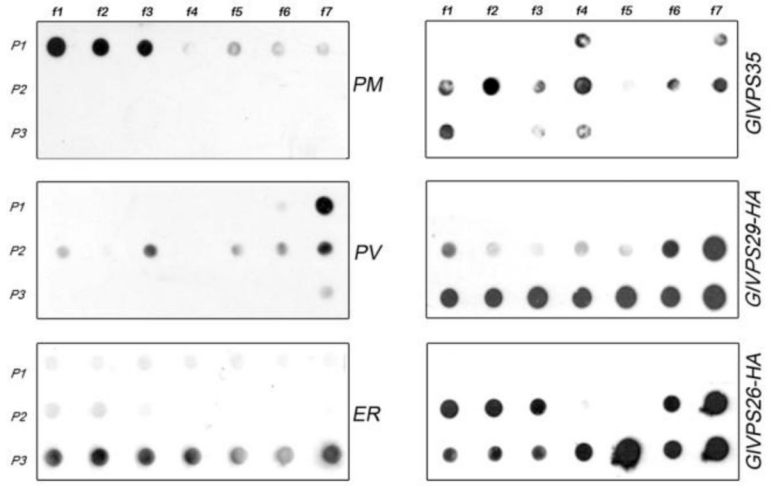

Figure 4. Sedimentation velocity analysis of retromer subunits

Lysates of *wild-type* or transgenic trophozoites were sequentially centrifuged at 1000 x g (P1), 20.000 x g (P2), and 105.000 x g (P3), the P3 supernatant applied on a sucrose gradient and fractionated by centrifugation. The fractions were analyzed by dot-blotting with antibodies to VSP1267 for plasma membrane (PM), BiP for ER, and μ2 for PV (left panels). GlVPS35 is found in fractions corresponding to the PVs and also to ER and PM. Anti-HA immunoreactivity shows GlVPS29-HA and GlVPS26-HA in fractions of ER but, interestingly, in high amounts in the PV fractions (right panels). Blots from representative experiments are shown.

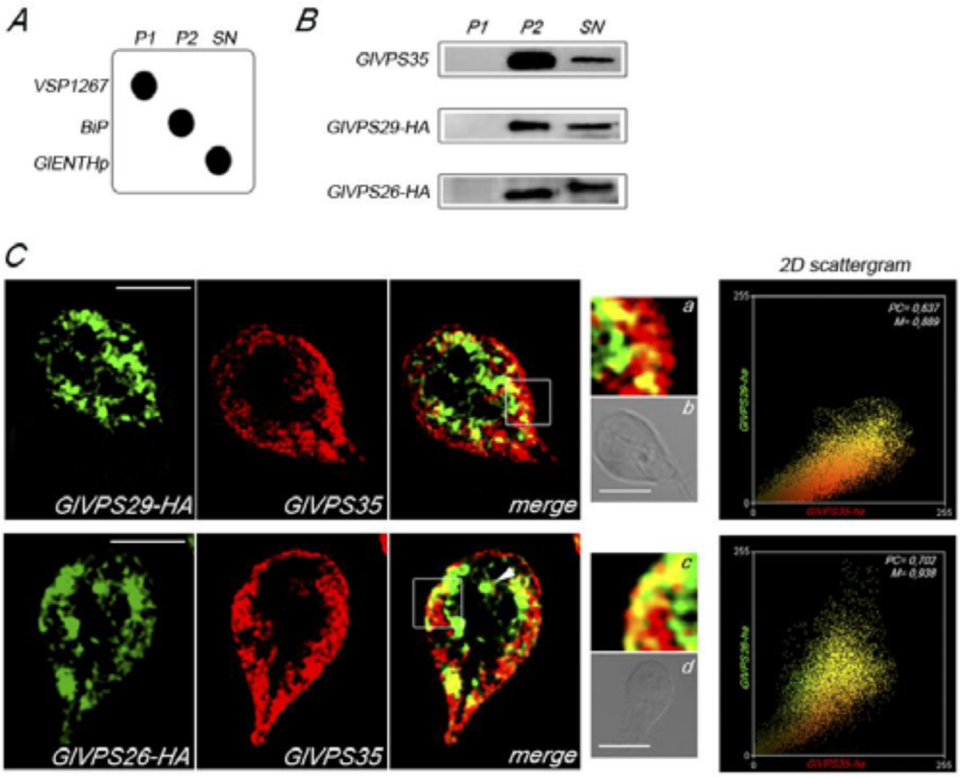

Figure 5. Membrane association of the GlVPSs

(A) Dot-blot analysis of VSP1267, BiP and GlENTHp, for plasma membrane (P1), microsomal (P2) and cytosol (SN) [Feliziani and Touz, unpublished results] markers, respectively. (B) Immunoblottingusing *wild-type* or transgenic trophozoites show that GlVPS35, GlVPS29-HA and GlVPS26-HA are present in the microsomal (P2) and cytosolic (SN) fractions. (C) Direct IFA and confocal microscopy using the anti-GlVPS35 pAb (red) or Alexa 488-anti-HA mAb to detect GlVPS29-HA and GlVPS26-HA (green) show partial colocalization of the subunits in some PVs (inset) and BZ (arrowead). All images were equally processed. Bars, 5 μm. Inset magnifies a region of the cell where the green and red fluorescence partially overlap (a and c). Differential interference contrast microscopy (b and d) is shown also as insert. 2D scattergram of the two labels confirms the colocalization (right panels). Pearson's coefficient (PC). Mander's Overlap coefficient (M). Coefficient data were obtained from all counted cells (n=50). One representative image of each IFA assay is shown as example.

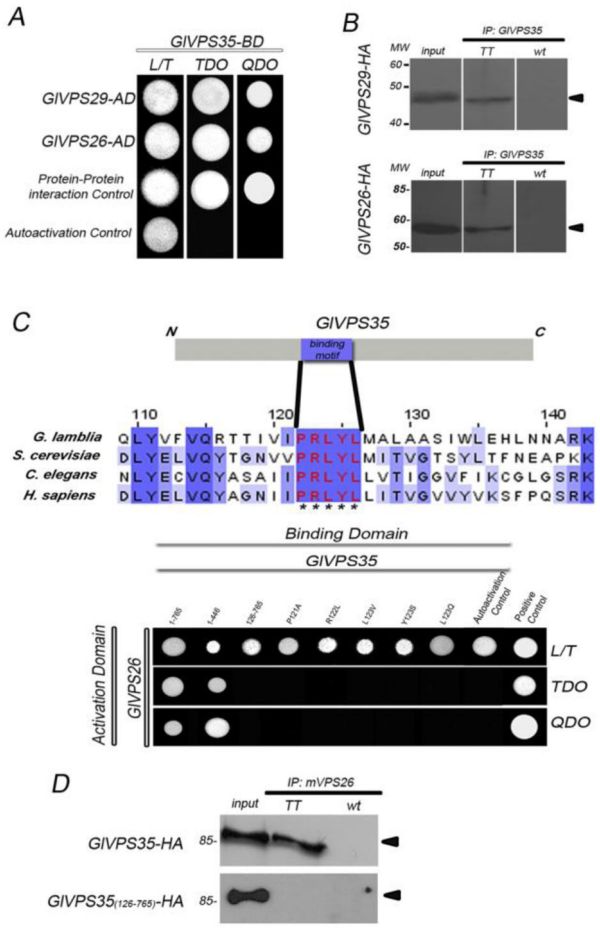

Figure 6. Interaction between the subunits

(A) The yeast two-hybrid assay demonstrates that GlVPS35 (GlVPS35-BD) interacts with GlVPS29-AD and GlVPS26-AD. Interaction is noticed by the growth of yeast colonies in plates lacking tryptophan, leucine and histidine [TDO (triple-dropout medium) plates] and in the high-stringency medium that also lacked adenine (QDO). Controls of the methodology include testing of pESCP-AD/pμ1-BD (protein-protein interaction) and pGlVPS35-BD/pGADT7 (autoactivation). (B) GlVPS35 interaction with GlVPS29 and GlVPS26 was confirmed by immunoprecipitation. GlVPS29-HA or GlVPS26-HA were co-immunoprecipitated together with GlVPS35 (arrowheads) from *glvps29-ha* or *glvps26-ha* transgenic (TT) but not from *wild-type* trophozoites (wt) by using the anti-GlVPS35 pAb. (C) Schematic representation of GlVPS35 illustrating the presence of the $_{122}$PRLYL$_{126}$ motif at N-terminal domain. Amino acid sequence alignment of the N-terminus of *G. lamblia*, *S. cerevisiae*, *C. elegans*, and *H. sapiens* Vps35 showed the conservation of the PRLYL motif. Alignment was performed using CLUSTAL 2.1 (http://www.clustal.org/clustal2/) with manual adjustment. Strictly conserved residues are highlighted in red and asterisks (*) while conserved amino acids are shown in blue and light blue. Yeast two-hybrid analyses showing the interaction of full-length and N-terminus of GlVPS35 (GlVPS35$_{1–765}$ and GlVPS35$_{1–448}$, respectively) with GlVPS26 but not with the N-terminus truncated GlVPS35 (GlVPS35$_{126–765}$) or GlVPS35 mutated in any of the aa composing the PRLYL conserved motif. Interaction of the fusion proteins was detected by growth of cotransformed cells in the TDO and QDO medium as described in the Materials and Methods. Controls are the same as in (A). (D) Immunoblotting showing that the anti-

mVPS26 pAb was able to coprecipitate GlVPS35-HA but not GlVPS35$_{126–765}$-HA together with GlVPS26.

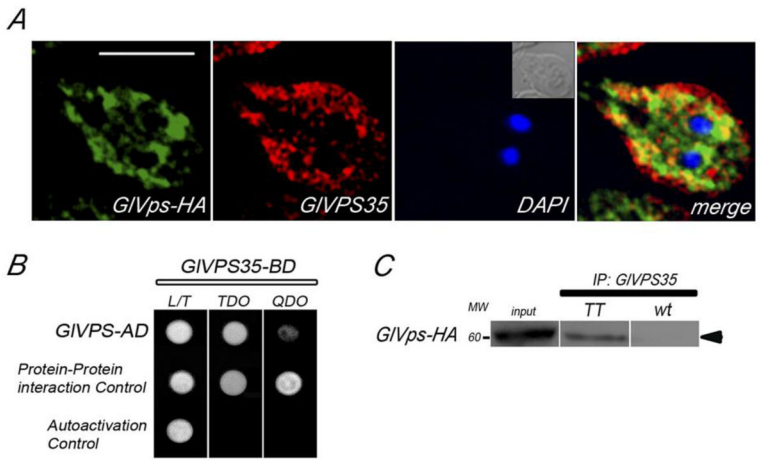

Figure 7. Interaction of GlVPS35 with the receptor GlVps

(A) Direct IFA and confocal microscopy show the colocalization (yellow in merge) of GlVps-HA (green) and GlVPS35 (red) using directed labeled anti-HA and anti-GlVPS35 Abs, respectively. Nuclear DNA was labeled with DAPI (blue). Differential interference contrast microscopy is shown as insert. Bar, 5 μm. (B) GlVps/GlVPS35 interaction was detected by the ability of yeast cells (AH109) to grow on selective plates TDO. No interaction was observed in the high-stringency QDO medium. Controls of the methodology include testing of pESCP-AD/pμ1-BD (protein-protein interaction) and pGlVPS35-BD/pGADT7 (autoactivation). (C) Coimmunoprecipitation of GlVps-HA and GlVPS35 using anti-GlVPS35 pAb confirm their interaction. Molecular weights of protein standards (kDa) are indicated on the left.

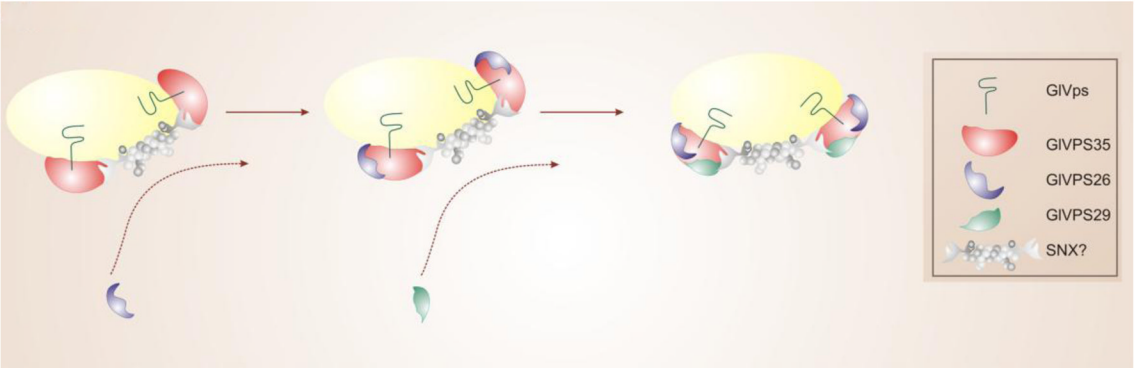

Figure 8. Working model for the assembly of the retromer complex

In this model, non-Snx-BAR proteins are associated to the endosomal membranes through the interactions between their PX domain and membrane phospholipids. GlVPS35, associates with the receptor cargo GlVps and sequentially recruiting GlVPS26 and GlVPS29. The final assembly of the retromer complex takes place in particular membrane domains.